



## Supplementary Materials for

### **Enhancing Depression Mechanisms in Midbrain Dopamine Neurons Achieves Homeostatic Resilience**

Allyson K. Friedman<sup>1</sup>, Jessica J. Walsh<sup>1,2</sup>, Barbara Juarez<sup>1,2</sup>, Stacy M. Ku<sup>1,2</sup>, Dipesh Chaudhury<sup>1</sup>, Jing Wang<sup>3</sup>, Xianting Li<sup>3</sup>, David M. Dietz<sup>4</sup>, Nina Pan<sup>3</sup>, Vincent F. Vialou<sup>4</sup>, Rachael L. Neve<sup>5</sup>, Zhenyu Yue<sup>3,4</sup>, Ming-Hu Han<sup>1,4\*</sup>

correspondence to: [Ming-Hu.Han@mssm.edu](mailto:Ming-Hu.Han@mssm.edu)

#### **This PDF file includes:**

Materials and Methods  
Figs. S1 to S14

## **Materials and Methods**

### Chronic social defeat and social interaction.

Chronic social defeat and avoidance testing were performed according to published protocols and our previous work (1, 9, 10, 13). During each defeat episode, male tyrosine hydroxylase TH-GFP or TH-Cre C57BL/6J 8 week old mice were exposed to a 10 min physical bout of interaction with an aggressive CD1 mouse. For the remainder of the time the C57 mouse is housed across a clear plexiglass divider providing further stressful sensory cues from the CD1 mouse. After the 10-day social defeat the C57 is singly housed. 24 hr following defeat the C57 undergoes a social interaction test with a novel CD1 aggressor. The social interaction test, measured the time spent in the interaction zone during the first (target absent) and second (target present) trials; the interaction ratio (IR) was calculated as  $100 \times [(\text{interaction time, target present})/(\text{interaction time, target absent})]$ . Behavioral phenotyping on days 11 and following re-test were performed. Defeated mice with  $IR < 100$  were defined as susceptible mice; other defeated mice are used as the resilient subgroup.

### Electrophysiology.

All recordings were carried out blind to the experimental conditions of behavioral, drug and viral treatment. Acute brain slices of VTA were prepared as done in previous studies (9, 12, 24, 34). Male TH-GFP, TH-Cre or C57BL/6J 11-15 week old mice were perfused with cold artificial cerebrospinal fluid (aCSF) containing (in mM): 128 NaCl, 3 KCl, 1.25  $\text{NaH}_2\text{PO}_4$ , 10 D-glucose, 24  $\text{NaHCO}_3$ , 2  $\text{CaCl}_2$ , and 2  $\text{MgCl}_2$  (oxygenated with 95%  $\text{O}_2$  and 5%  $\text{CO}_2$ , pH 7.35, 295–305 mOsm). Acute brain slices (250  $\mu\text{m}$ ) containing the VTA were cut using a microslicer in sucrose-ACSF, which was derived by fully replacing NaCl with 254 mM sucrose, and saturated by 95%  $\text{O}_2$  and 5%  $\text{CO}_2$ . Slices were maintained in the holding chamber for 1 hr at 37°C. Slices were transferred into a recording chamber fitted with a constant flow rate of aCSF equilibrated with 95%  $\text{O}_2$ /5%  $\text{CO}_2$  (2.5 ml/min) and at 35°C. Glass microelectrodes (2-4  $\text{M}\Omega$ ) filled with an internal solution containing (mM): 115 potassium gluconate, 20 KCl, 1.5  $\text{MgCl}_2$ , 10 phosphocreatine, 10 HEPES, 2 magnesium ATP, and 0.5 GTP (pH 7.2, 285 mOsm). VTA DA neurons were identified by their location and infrared differential interference contrast microscopy and recordings were made from TH-GFP positive neurons, eYFP

positive neurons for viral and optogenetic experiments and lumafluor positive neurons for projection-specific recordings (Fig. 1 to 4)(9). Electrophysiological properties were evaluated from whole-cell recordings as shown in fig. S2. Duration was determined from half amplitude from threshold to peak. Firing rate was recorded with cell-attached configuration (1, 9). Whole-cell voltage-clamp was used to record  $I_h$  current with a series of 3 s pulses with 10 mV command voltage steps from -130 mV to -70 mV from a holding potential at -70 mV (12). To isolate voltage-gated  $K^+$  channel-mediated currents, 4 s pulses with 10 mV step voltages from -70 to +20 at -70 holding potential were used in the presence of aCSF containing 1  $\mu$ M tetrodotoxin, 200  $\mu$ M  $CdCl_2$ , 1mM kynurenic acid, and 100  $\mu$ M picrotoxin as performed in our previous study (24, 34). Cell excitability was measured with 2 s incremental steps of current injections (50, 100, 150, and 200 pA) (9). Series resistance was monitored during all recordings.

#### Cannula surgery and micro-infusion of lamotrigine into the VTA.

24 hr after social interaction test mice were placed under a combination of ketamine (100 mg/kg)/xylazine (10 mg/kg) anesthesia before bilateral stereotaxic implantation of 26 gauge guide cannula fitted with obturators that were secured to the skull after being positioned 1 mm directly above the VTA (AP, -3.2; ML, 0.4; DV, -3.7 mm; 0° angle) as described previously (9, 12). After 5 days of postoperative recovery, simultaneous bilateral microinjections of lamotrigine (0.1  $\mu$ g) or vehicle (phosphate-buffered saline, PBS) was delivered through an injector cannula in a total volume 0.4  $\mu$ l/side at a continuous rate of 0.1  $\mu$ l/min under the control of a micro-infusion pump. Concentration was selected based on published studies and on validation of *in vitro* effects on DA neuron activity in this study (16). Injector cannulas were removed 5 min after the stopping of each infusion to prevent backflow. Cannula placements were confirmed postmortem in all animals.

#### Sucrose preference.

For 2-bottle choice sucrose-preference testing, a solution of 1% sucrose or drinking water was filled in two 50 ml tubes with stoppers fitted with ball-point sipper tubes as described previously (1, 9). All animals were singly-housed and acclimatized to two-bottle choice conditions prior to testing conditions. 12 hr or 24 hr post treatment, fluid was weighed

and the positions of the tubes were interchanged. Sucrose preference was calculated as a percentage [ $100 \times (\text{volume of sucrose consumed (in bottle A)}/\text{total volume consumed (bottles A and B)})$ ].

#### Forced swim test.

The forced swim test (FST) was performed as previously described (7). 4 days post viral injection or 24 hour post optogenetic stimulation mice were placed for 6min in a 4 liter Pyrex glass beaker containing 3 liters of water at  $24 \pm 1^\circ\text{C}$ . Water was changed between subjects. All test sessions were recorded by a digitally tracking Ethovision positioned on the side of the beaker. Time spent immobile was independently analyzed by Ethovision software. A decrease in immobility time indicates an antidepressant-like response (7).

#### Immunohistochemistry.

Mice were fully anesthetized with ketamine (100mg/kg) with xylazine (10mg/ml) mixture before the vascular perfusion as described previously (1,9). Mice were perfused with 30ml cold PBS and 30ml 4% paraformaldehyde (PFA). Brain tissue were removed and post-fixed with 4% PFA, then treated with 30% sucrose at  $4^\circ\text{C}$  for two days. The VTA region of the brain were sliced on the cryostat, the sections were collected consecutively and preserved into antifreeze buffer (30% Glycerin solution in ethylene glycol) at  $-20^\circ\text{C}$ . Brain tissue was sectioned with thickness of  $30\mu\text{m}$  and sections were stored in  $4^\circ\text{C}$  in PBS and sodium azide until IHC. For immuno-staining and quantification of VTA DA neurons, serial sections representing the rostral to caudal extent of the VTA were selected for analysis. Brain sections were rinsed 3X with PBS and blocked with blocking buffer (5% goat serum, PBS with 0.2% Triton X-100) for 1 hr. Sections were incubated with primary Anti-TH (Sigma, 1:10,000) and anti-GFP (Invitrogen, 1:2000) monoclonal antibody at  $4^\circ\text{C}$  for 24 hr. The next day sections were incubated with secondary antibody (Alexa Fluor 488, Goat x mouse IgG) for 2 hr. Sections were then rinsed with PBS 3 times before mounting on the slide (9, 24). Sections were subsequently imaged ( $\times 20$  magnification) on a LSM 710 confocal (Zeiss). Cell counting was carried out manually using ImageJ.

#### Virus vectors.

AAV-DIO-ChR2-eYFP and AAV-DIO-eYFP virus plasmids were purchased from University of North Carolina vector core facility (UNC). HSV-LS1L-HCN2-eYFP and

HSV-LS1L-eYFP were provided by Rachael Neve's laboratory in Massachusetts Institute of Technology (MIT). An AAV2/5 vector that undergoes retrograde transport, expressing Cre (AAV2/5-Cre) was used in this study for targeting VTA-NAc pathway and VTA-mPFC pathway, respectively. The vector was purchased from University of Pennsylvania Vector Core.

#### Stereotaxic surgery, viral-mediated gene transfer, and optic fiber placement.

The related procedures were performed as described previously (9, 23, 24). TH-Cre mice were anesthetized with ketamine (100mg/kg)/xylazine (10mg/kg) mixture, placed in a stereotaxic apparatus and their skull was exposed by scalpel incision. For viruses, thirty-three gauge needles were placed bilaterally at 7° angle into the VTA (AP -3.3; LM +1.0; DV -4.6 in the mm) and 0.5 µl of virus was infused at a rate of 0.1 µl/min as performed in our previous study (9, 23, 24). We utilized the chronic implantable optical fiber system as performed in our previous studies (9, 23). Chronically implantable fibers were made with 200 µm core optic fiber and light output through the optical fibers was measured prior to bilateral implantation. Fibers measuring at least 10 mW were utilized. They were implanted into the VTA at a 7° angle (AP -3.3 mm; LM +1.0 mm; DV -4.4 mm) and secured to the skull with industrial strength dental cement. Implantable optical fibers ensure that the same tissue is repeatedly stimulated. Optical fiber placements were confirmed postmortem in all animals.

#### Projection-specific manipulations.

To selectively target either the NAc or mPFC projecting VTA neurons we used a combination of a retrograding AAV2/5-Cre injected in to either site, and Cre inducible virus AAV-DIO-ChR2-eYFP or HSV-LS1L-HCN2-eYFP injected into the VTA. Retrograding AAV2/5-Cre was injected to the NAc (bregma coordinates: AP, +1.5; LM, +1.6; DV, -4.4; 10° angle) or mPFC (bregma coordinates: AP, +1.7; LM, +1.6; DV, -2.5; 15° angle), and Cre-inducible AAV-DIO-ChR2-eYFP or HSV-LS1L-HCN2-eYFP to the VTA. Therefore, ChR2 or HCN2 was expressed selectively in NAc or mPFC projecting neurons in the VTA.

#### Blue light stimulation.

To selectively activate the DA neurons in the VTA, cell-type specific expression of ChR2 was realized by combined use of TH-Cre mice and Cre-inducible AAV-DIO-ChR2-eYFP

(University of North Carolina). While this viral vector and mouse line were successfully used in our previous work (9, 23), morphological and functional validations were further performed in this study. 473 nm blue laser diode and a stimulator were used to generate blue light pulses as described previously (9, 23). For *in vitro* slice electrophysiological validation of ChR2 activation we tested 0.1-50 Hz stimulation protocols. For all *in vivo* behavioral experiments, mice were given, high frequency, phasic (20 Hz, 40 ms; 80% duty cycle) light stimulations (9). This protocol was established based on *in vivo* studies that showed an increase in overall firing as well as burst firing in VTA DA neurons in susceptible animals (12).

#### Statistics.

Unless otherwise noted, we used two-tailed unpaired Student's t tests (for comparison of two groups), one-way analysis of variance (ANOVA) followed by *t*-test comparison (for three groups).

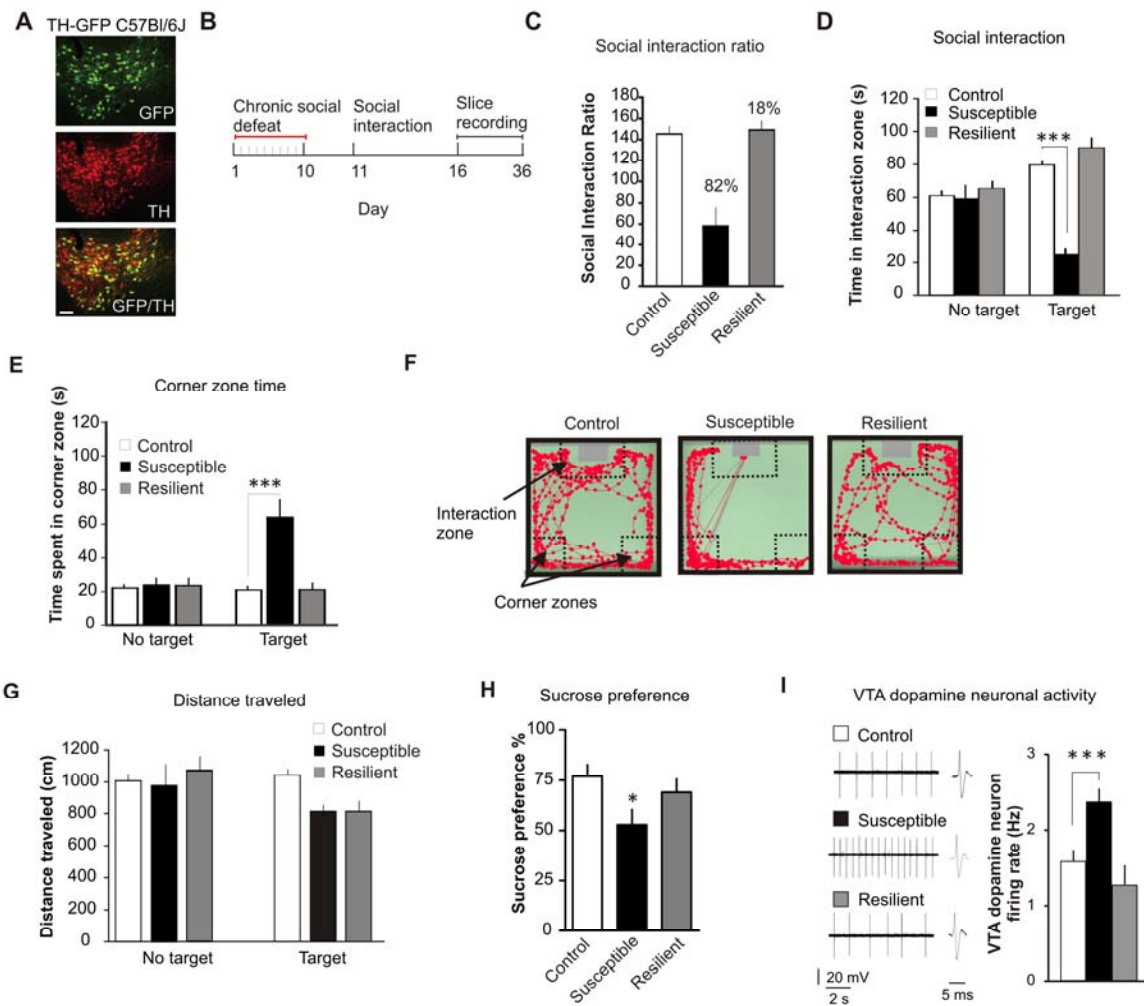


**Fig. S1.** Determination, distribution and behavior of susceptible and resilient subgroups following 10-day social defeat paradigm. **(A)** Confocal image of immuno-staining for TH in TH-GFP mice. Quantification shows:  $72.3\% \pm 2.15$  of VTA neurons were TH<sup>+</sup>,  $54.2\% \pm 6.22\%$  were eYFP<sup>+</sup>, and  $97\% \pm 1.0\%$  of the TH neurons were also labeled with eYFP (2-3 sections per mouse; data from 5 animals). Scale bar, 100  $\mu$ m; green, GFP; red, TH. **(B)** Experimental timeline. **(C)** Social interaction ratio, and percentage breakdown of mice in either susceptible or resilient subgroup. **(D)** Social interaction time ( $F_{(2,53)} = 107.87$ ,  $P < 0.0001$ ,  $n = \text{control:30, susceptible:14, resilient:10}$ ). **(E)** Time spent in corner zone during social interaction test is significantly increased in susceptible mice ( $F_{(2,53)} = 21.10$ ,  $P < 0.0001$ ;  $n = \text{control:30, susceptible:14, resilient:10}$ ). **(F)** Representative traces of mouse behavior during social interaction test after having undergone chronic social

defeat 24 hr earlier. **(G)** Distance traveled is not significantly different between phenotypes ( $F_{(2,53)} = 0.26$ ,  $P = 0.77$ ;  $n = \text{control:30, susceptible:14, resilient:10}$ ). **(H)** Sucrose preference is significantly reduced in the susceptible subgroup compared to control and resilient ( $F_{(2,35)} = 3.42$ ,  $P < 0.05$ ;  $n = 12$ ). **(I)** Baseline DA neuron firing frequency of VTA brain slices from TH-GFP control, susceptible and resilient mice after chronic (10-day) social defeat ( $F_{(2,37)} = 7.24$ ,  $P < 0.001$ ,  $n = 12-14$ ). Error bars,  $\pm$  s.e.m. \*  $P < 0.05$ , \*\*\*  $P < 0.001$ .



Comparison of electrophysiological properties

	Membrane potential (mV)	Threshold (mV)	Peak (mV)	Duration (ms)	Afterhyperpolarizations (mV)
□ Control	-55.4 ± 0.85	-37.7 ± 1.0	16.4 ± 6.5	0.76 ± 0.03	-63.7 ± 2.8
■ Susceptible	-56.6 ± 0.89	-36.4 ± 1.2	16.6 ± 4.3	0.75 ± 0.06	-64.6 ± 1.9
■ Resilient	-55.5 ± 1.22	-37.9 ± 1.1	15.5 ± 6.2	0.76 ± 0.05	-63.9 ± 1.6

**Fig. S2.** Control, susceptible and resilient VTA GFP<sup>+</sup> DA neurons show no significantly different electrophysiological properties. Membrane potential:  $F_{(2,74)} = 0.48$ ,  $P = 0.62$ ; Action potential threshold:  $F_{(2,74)} = 0.98$ ,  $P = 0.38$ ; Action potential peak:  $F_{(2,74)} = 0.16$ ,  $P = 0.85$ ; Action potential duration  $F_{(2,74)} = 1.93$ ,  $P = 0.15$ ; Afterhyperpolarization  $F_{(2,74)} = 0.94$ ,  $P = 0.40$ . (n = 25 cells/ 5 mice per group).

## Homeostatic resilience

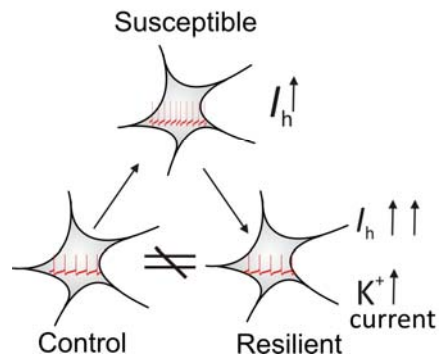


**Fig. S3.** Schematic model summary of behavioral, physiological and ionic findings. The resilient phenotype shows control-level activity of VTA dopamine neurons, a stabilized firing status established by a new balance of  $I_h$  and  $K^+$  channel currents.

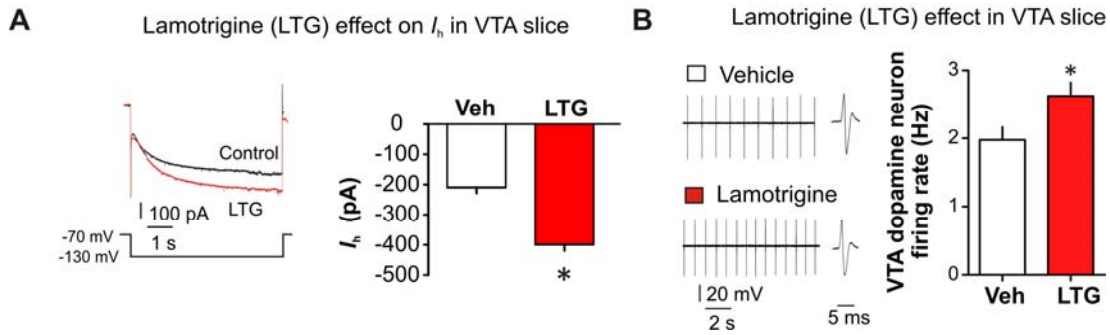


**Fig. S4.** Lamotrigine increases  $I_h$  current and the firing rate of VTA dopamine neurons in brain slice preparation. **(A and B)** Lamotrigine perfusion *in vitro* significantly increases both VTA DA neuron  $I_h$  current ( $t_{13} = 2.84$ ,  $P < 0.05$ ) and firing rate ( $t_{13} = 2.60$ ,  $P < 0.05$ ;  $n = 7-8$ ). Error bars,  $\pm$  s.e.m. \*  $P < 0.05$ .

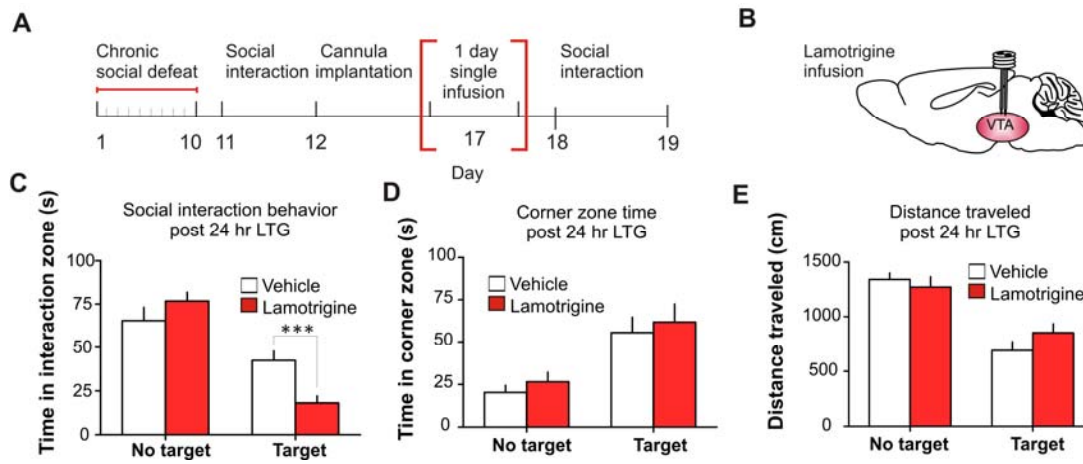


**Fig. S5.** A single infusion of  $I_h$  potentiator lamotrigine enhances social avoidance in susceptible mice. (**A** and **B**) Experimental timeline: following a 5 day recovery from bilateral VTA cannula surgery mice, susceptible mice received single dose infusion and behavioral testing. (**C**) Social interaction behavior post infusion of lamotrigine in susceptible mice increases social avoidance ( $t_{14} = 4.48$ ,  $P < 0.001$ ,  $n = 8$ ). (**D**) Corner zone time is not altered ( $t_{14} = 0.66$ ,  $P = 0.52$ ,  $n = 8$ ). (**E**) Locomotion activity is not altered post a single administration of lamotrigine or vehicle ( $t_{14} = 1.31$ ,  $P = 0.213$ ,  $n = 8$ ). Error bars,  $\pm$  s.e.m. \*\*\*  $P < 0.001$ .

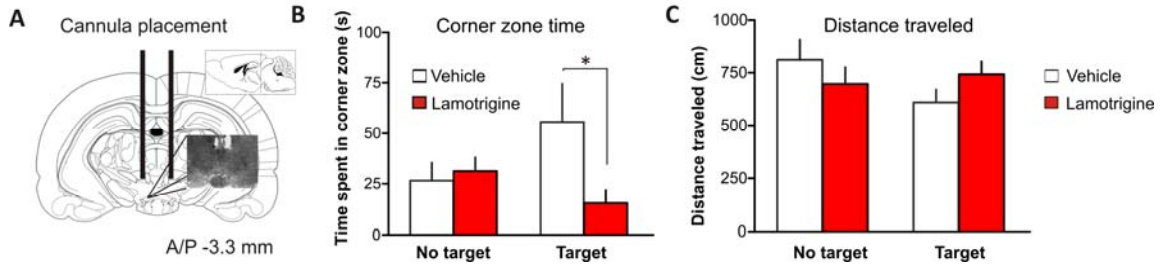


**Fig. S6.** Repeated infusion of lamotrigine to the VTA of susceptible animals decreases the time spent in the corner zone and does not alter distance traveled. **(A)** Schematic coronal sections from VTA (adapted from Allen Brain Atlas) with an inset of sample crystal violet stain of VTA bilateral cannula placement used in micro-infusion experiment. Accurate injection sites were confirmed in all animals post-mortem. **(B)** Corner zone time is decreased ( $t_{18} = 2.67$ ,  $P < 0.05$ ;  $n = 10$ ). **(C)** Locomotor activity is not altered following chronic infusion of lamotrigine ( $t_{18} = 1.71$ ,  $P = 0.11$ ;  $n = 10$ ). Error bars,  $\pm$  s.e.m. \*  $P < 0.05$ .

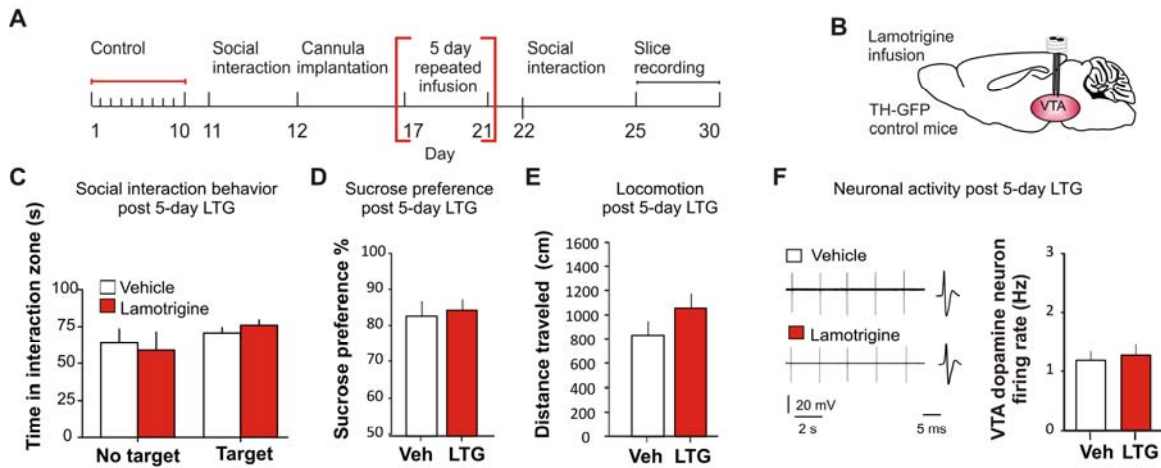


**Fig. S7.** Repeated infusion of  $I_h$  potentiator lamotrigine to the VTA of control mice does not alter social behavior or neuronal activity (**A**) Experimental timeline. (**B**) Schematic of lamotrigine infusion into the VTA of stress naïve control TH-GFP mice. (**C**) 5 days of 3 min daily bilateral infusions of lamotrigine (LTG, 0.1  $\mu$ g) or vehicle into the VTA does not alter social interaction time ( $t_{16} = 0.31$ ,  $P = 0.76$ ;  $n = 9$ ), (**D**) sucrose preference ( $t_{16} = 0.44$ ,  $P = 0.67$ ;  $n = 9$ ) or (**E**) distance traveled ( $t_{16} = 1.74$ ,  $P = 0.10$ ;  $n = 9$ ). (**F**) Sample traces and statistic data of VTA DA neuron firing in control mice following repeated infusion of vehicle compared to lamotrigine ( $t_{22} = 0.50$ ,  $P = 0.62$ ;  $n = 12$  cells/6 mice per group). Error bars,  $\pm$  s.e.m.

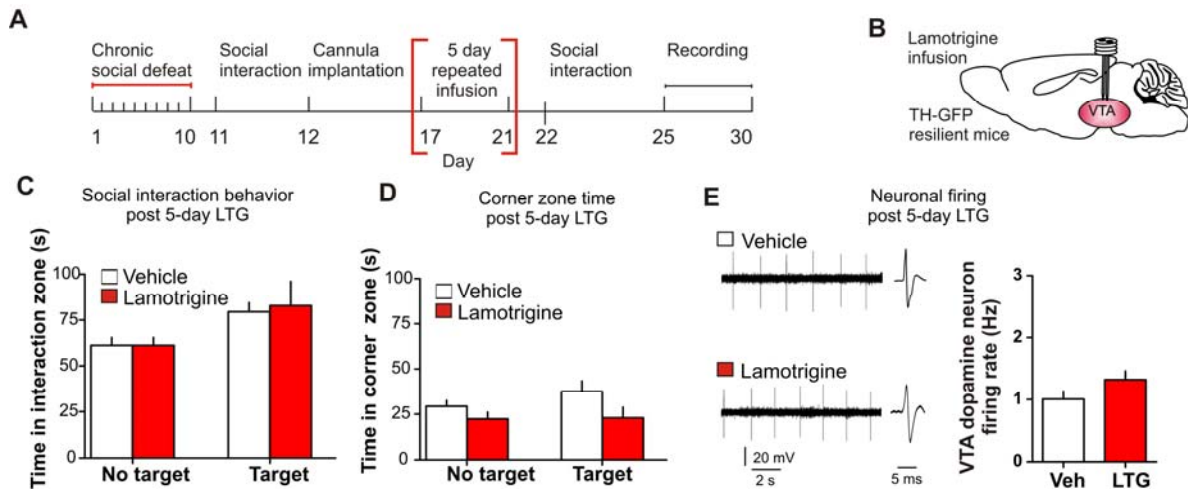


**Fig. S8.** Repeated infusion of  $I_h$  potentiator lamotrigine to the VTA of resilient mice does not alter social behavior or neuronal activity (**A**) Experimental timeline. (**B**) Schematic of lamotrigine infusion into the VTA of resilient TH-GFP mice. (**C**) 5 day of 3 min daily bilateral infusions of lamotrigine (0.1  $\mu$ g) or vehicle into the VTA does not alter social interaction time ( $t_{10} = 0.24$ ,  $P = 0.82$ ;  $n = 6$ ) or (**D**) corner zone time ( $t_{10} = 1.74$ ,  $P = 0.11$ ;  $n = 6$ ). (**E**) Sample traces and statistic data of VTA dopamine neuron firing in control mice following repeated infusion of vehicle compared to lamotrigine ( $t_{46} = 1.86$ ,  $P = 0.10$ ;  $n = 24$  cells/5 mice per group). Error bars,  $\pm$  s.e.m.

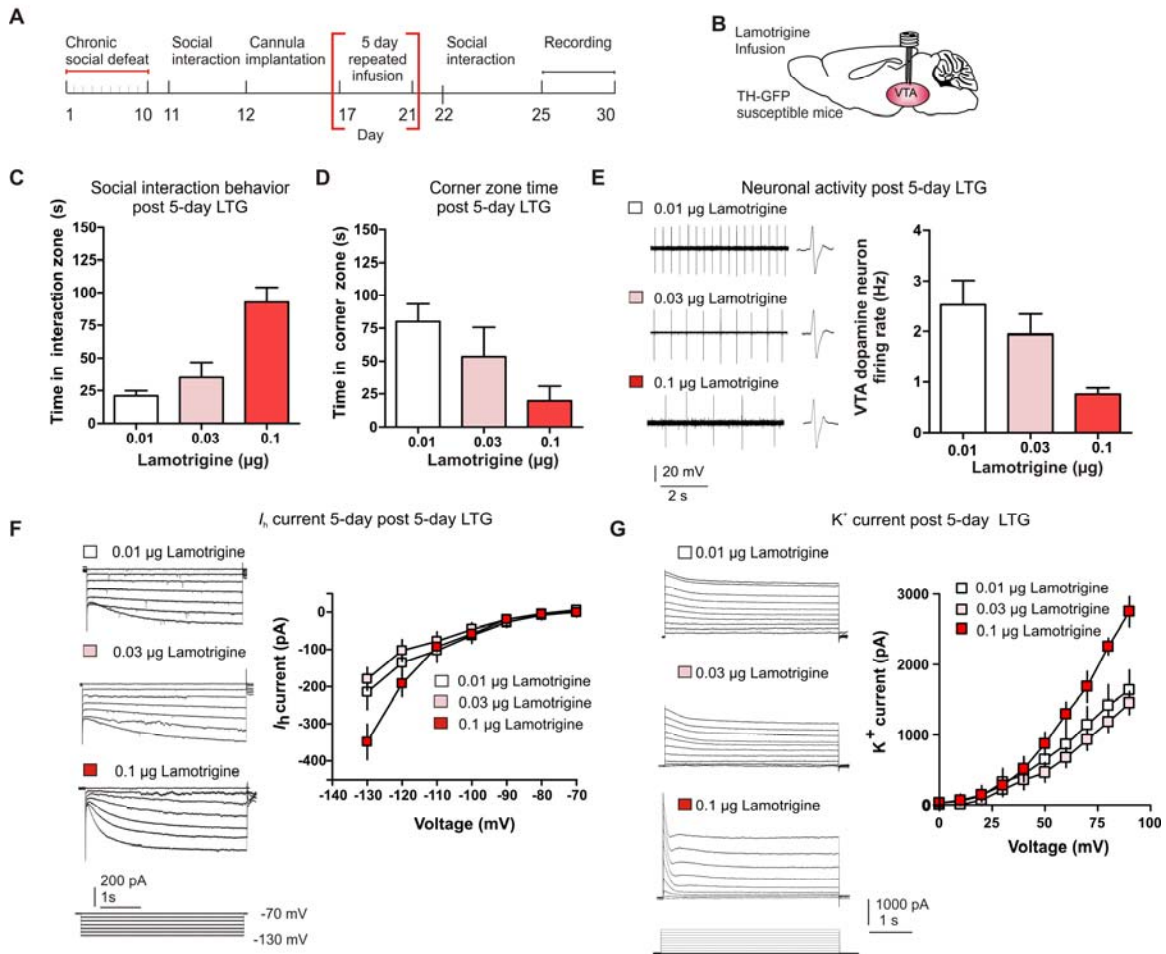


**Fig. S9.** Dose response of repeated lamotrigine infusion to the VTA of susceptible mice. **(A)** Experimental timeline. **(B)** Schematic of lamotrigine infusion into susceptible TH-GFP mice. **(C)** Social interaction time and **(D)** corner zone time with target following 5 day infusion of lamotrigine at 0.01  $\mu\text{g}$ , 0.03  $\mu\text{g}$  and 0.1  $\mu\text{g}$  concentration ( $n = 5$ ). **(E)** Sample traces and group data of firing rate following the 5 day infusion of lamotrigine at 0.01  $\mu\text{g}$ , 0.03  $\mu\text{g}$  and 0.1  $\mu\text{g}$  concentrations, ( $n = 5$  cells/ 3 animals per group). **(F)** Sample traces and group data of  $I_h$  following the 5 day infusion of lamotrigine at 0.01  $\mu\text{g}$ , 0.03  $\mu\text{g}$  and 0.1  $\mu\text{g}$  concentrations ( $n = 6-7$  cells/ 3 animals per group). **(G)** Sample traces and group data of  $K^+$  channel currents following the 5 day infusion of lamotrigine at 0.01  $\mu\text{g}$ , 0.03  $\mu\text{g}$  and 0.1  $\mu\text{g}$  concentrations ( $n = 5-6$  cells/ 3 animals per group). Error bars,  $\pm$  s.e.m.



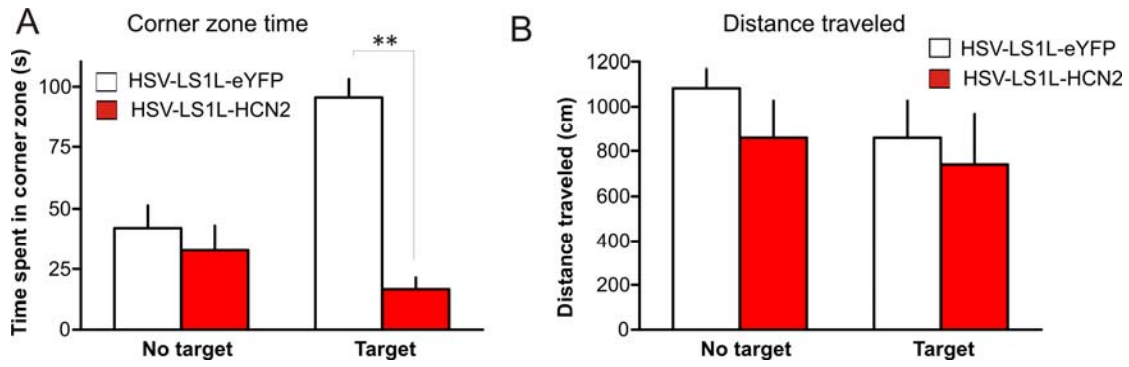


**Fig. S10.** Overexpression of HCN2 channels in TH<sup>+</sup> neurons of susceptible mice significantly reduces corner zone time and does not alter locomotor activity. **(A)** Corner zone time is decreased ( $t_{18} = 4.18$ ,  $P < 0.01$   $n = 10$ ) and **(B)** locomotor activity is not altered ( $t_{18} = 0.14$   $P = 0.89$ ;  $n = 10$ ) with target present. Error bars,  $\pm$  s.e.m. \*\*  $P < 0.01$ .

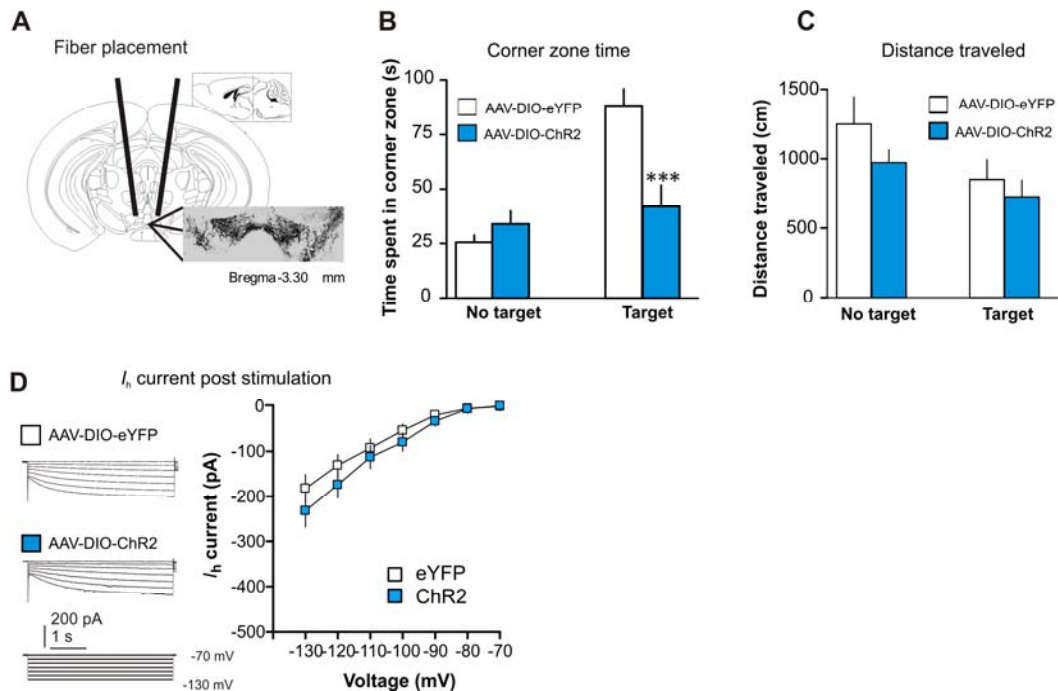


**Fig. S11.** Repeated optogenetic stimulation of VTA DA neurons significantly reduces corner zone time and does not alter locomotion or  $I_h$ . **(A)** Schematic coronal sections from VTA (adapted from Allen Brain Atlas) with an inset of sample crystal violet stain of VTA bilateral ferrule placement used in optogenetics experiment. Accurate stimulation sites were confirmed in all animals post-mortem. **(B)** In the presence of a social target, previously susceptible mice, injected with AAV-DIO-ChR2-eYFP and given chronic photo-activation 20 minutes a day for 5 days spent significantly less time in the corner zone compared to susceptible mice injected with control AAV-DIO-eYFP ( $t_{22} = 3.59$ ,  $P < 0.001$ ;  $n = 12$ ). **(C)** There was no difference in total distance traveled during the social interaction test ( $t_{22} = 1.03$ ,  $P = 0.32$ ;  $n = 12$ ). **(D)** Sample traces and statistic data of  $I_h$  show no change following photo-activation (At -130 pA:  $t_{27} = 1.148$ ,  $P = 0.261$ ;  $n = 14-15$  cells). Error bars,  $\pm$  s.e.m. \*\*\*  $P < 0.001$ .

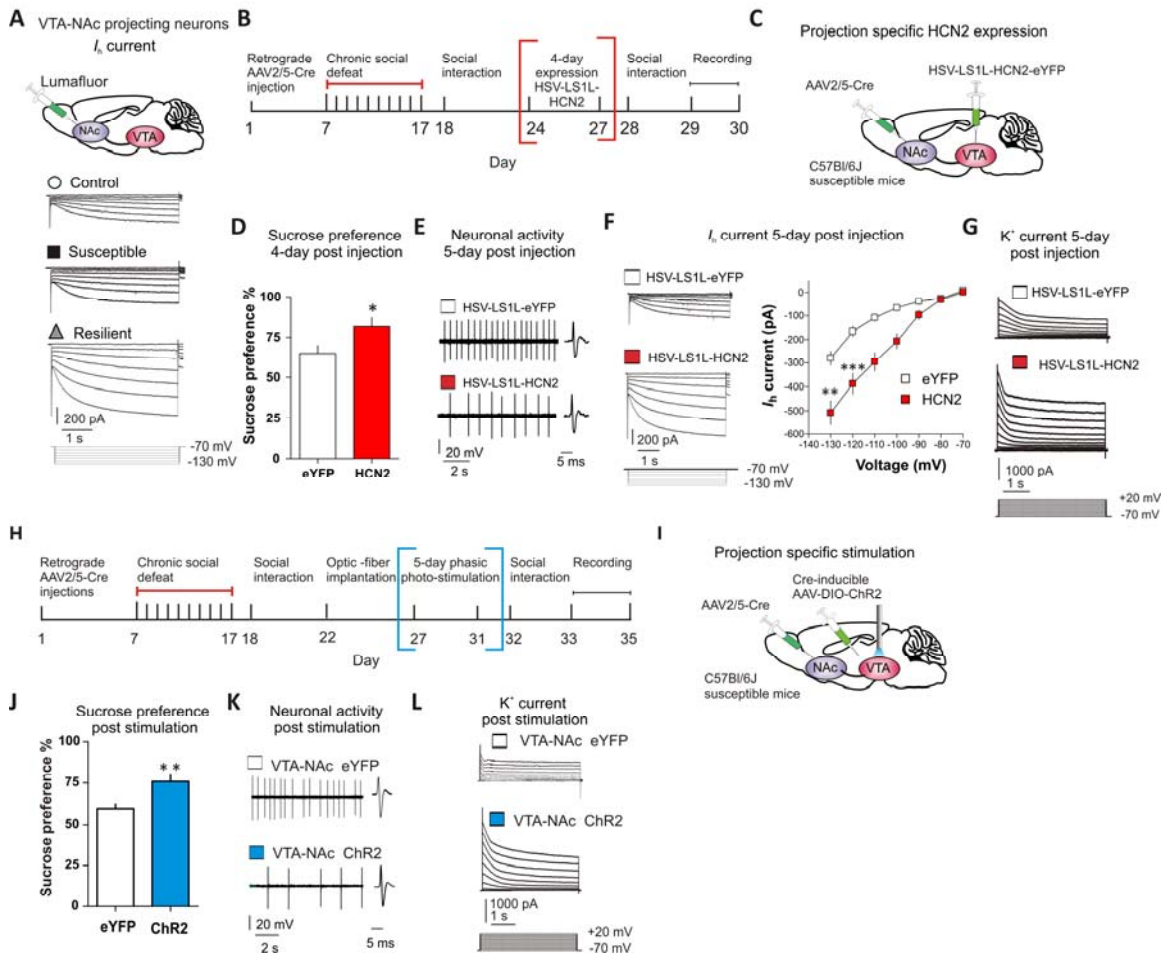


**Fig. S12.** The observed homeostatic plasticity is specific in  $I_h$ -presenting VTA-NAc projection. **(A)** Sample traces of  $I_h$  in VTA-NAc neurons labeled by lumafluor injection. **(B)** Experimental timeline. **(C)** Retrograding AAV2/5-Cre bilateral injection into the NAc and Cre-inducible HSV-LS1L-HCN2-eYFP bilateral injection into the VTA. **(D)** Sucrose preference test is significantly different post 4 day injection ( $t_{10} = 2.25$ ,  $P < 0.05$ ;  $n = 6$ ). **(E)** Sample traces firing activity of VTA-NAc neurons following expression of HCN2 virus. **(F)** Sample traces and statistic data of  $I_h$  increase in VTA-NAc neurons following expression of HCN2 virus (At -130 mV:  $t_{18} = 3.60$ ,  $P < 0.01$ ; -120 mV:  $t_{18} = 5.87$ ,  $P < 0.0001$ ;  $n = 10$  cells/6 mice per group). **(G)** Sample traces of peak  $K^+$  current of VTA-NAc neurons following expression of HCN2 virus. **(H)** Experimental timeline. **(I)** Retrograding AAV2/5-Cre bilateral injection into the NAc and Cre-inducible AAV-DIO-

ChR2 bilateral injection and optic-fiber implantation into the VTA. **(J)** Sucrose preference test is significantly different post 5 day stimulation ( $t_{20} = 3.25$ ,  $P < 0.01$ ;  $n = 11$ ). **(K)** Sample traces firing activity of VTA-NAc neurons post 5 day stimulation. **(L)** Sample traces of peak  $K^+$  current of VTA projecting NAc neurons post 5 day stimulation. Error bars,  $\pm$  s.e.m. \*  $P < 0.05$ , \*\*  $P < 0.01$ , \*\*\*  $P < 0.001$ .

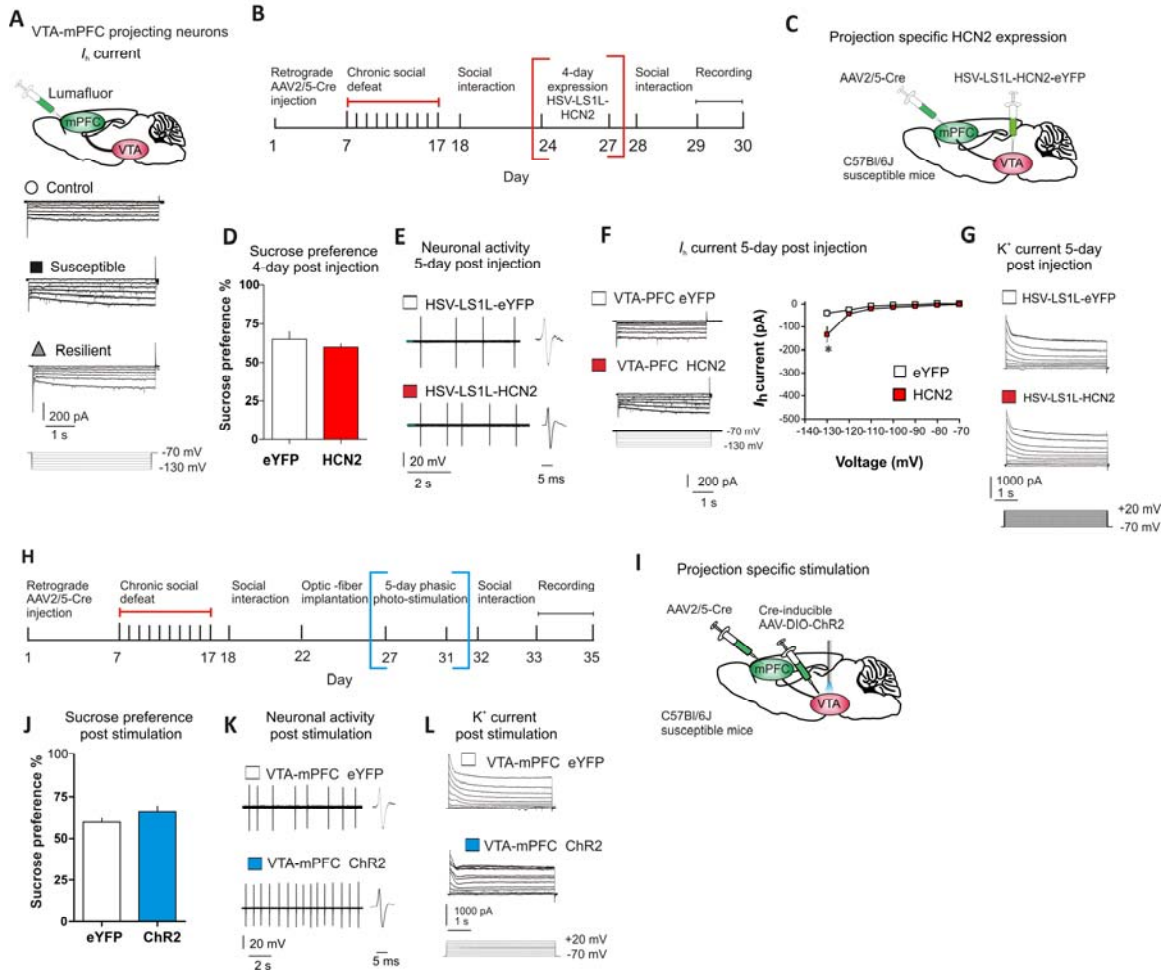


**Fig. S13.** mPFC projecting VTA neurons demonstrate  $I_h$ -independent plasticity. **(A)** Sample traces of  $I_h$  in VTA-mPFC neurons labeled by lumafluor injection. **(B)** Experimental timeline. **(C)** Retrograding AAV2/5-Cre bilateral injection into the mPFC and Cre-inducible HSV-LS1L-HCN2-eYFP bilateral injection into the VTA. **(D)** Sucrose preference test is not significantly different post 4 day injection ( $t_{18} = 0.36$ ,  $P = 0.72$ ;  $n = 10$ ). **(E)** Sample traces firing activity of VTA-mPFC neurons following expression of HCN2 virus. **(F)** Sample traces and statistic data of  $I_h$  in VTA-mPFC neurons following expression of HCN2 virus (At -130 mV:  $t_{18} = 2.12$ ,  $P < 0.05$ ;  $n = 10$  cells/5 mice per group). **(G)** Sample traces of peak  $K^+$  current of VTA-mPFC neurons following expression of HCN2 virus. **(H)** Experimental timeline. **(I)** Retrograding AAV2/5-Cre bilateral injection into the mPFC and Cre-inducible AAV-DIO-ChR2 bilateral injection and optic fiber implantation into the VTA. **(J)** Sucrose preference test is not significantly

different post 5 day stimulation. ( $t_{20} = 1.42$ ,  $P = 0.17$ ;  $n = 11$ ). **(K)** Sample traces firing activity of VTA-mPFC neurons post 5 day stimulation. **(L)** Sample traces of peak  $K^+$  current of VTA-mPFC neurons post 5 day stimulation. Error bars,  $\pm$  s.e.m. \*  $P < 0.05$ .

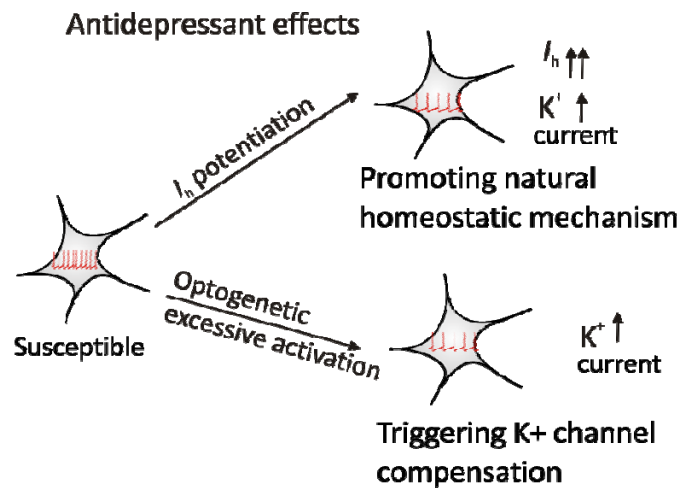


**Fig. S14.** Novel therapeutic strategy. Further increasing  $I_h$  in susceptible animals or excessive activation of already hyperactive VTA DA neurons subsequently induced a homeostatic compensatory up-regulation of  $K^+$  channel-mediated currents and established a more stable neuronal status, the same phenomenon observed in resilient mice.